GEOMETRICAL RECONSTRUCTION FOR THE NEW BUBBLE CHAMBERS

M. Aderholz, J. Bettels, F. Bruyant, H. Burmeister,
P. Dodd, E. Gelsema, W. Hart, J. Klopcic, W.G. Moorhead,
P. Laurikainen, A. Norton, M.C. Turnill, I. Wacek,
J. Derré*, A.-M. Lapassat*, D. Morellet**, and C. Pascaud**.

CERN, Geneva, Switzerland.

1. Introduction

The Large Bubble Chamber Geometry (LBCG) program being written at CERN in collaboration with other laboratories is primarily for Gargamelle, Mirabelle and the 3m70 Big European Bubble Chamber (BEBC), sketches of which are shown in Figure 1. There are some important aspects in which these chambers differ from classical ones as far as the reconstruction is concerned, and these are discussed in Section 1. Some typical artificial events for Gargamelle and BEBC are shown in Figures 2 and 3.

The LBCG program has been written in a modular fashion, so that alternative numerical methods can be employed. For example, different methods are required for hydrogen and heavy liquid. To achieve this modularity, the LBCG program has been designed around a flexible linked block data structure. This structure, and the functions of some of the more important modules, are outlined in Section 2.

This work, which is by no means complete, has also involved the writing of programs for the generation of artificial events, for the finding of camera positions, and for the fitting of magnetic field data. These programs are briefly outlined in Section 3.

Further details about all topics can be found in the LBCG Information Notes. Individual references to these Notes have not been given.

---

* Centre d'Etudes Nucléaires de SACLAY, France.

** Laboratoire d'Accélération Linéaire, Orsay, France.

1.1 Features of the new chambers affecting the reconstruction

In the three new bubble chambers considered, the cameras view the chamber through fish-eye lenses in contact with the liquid. These lens systems have angles of view going through 110^{o} and their calibration presents considerable problems. An optic axis in the usual sense does not exist, but an approximate axis of symmetry is chosen for each lens system and referred to by that name. In Gargamelle and BEBC the optic axes of the separate lens systems are considerably inclined with respect to each other.

In the case of Gargamelle and Mirabelle there are eight cameras and a given track may be measured on any sub-set of the eight. Tracks do not often project into circles in the film plane; in the limit a loop or cusp can appear. The vertex may not be visible in some views.

In all cases, it is difficult to establish a stable reference system of fiducial marks in the chamber. The crosses are attached to the walls of a chamber which is pulsating, and also they are seen through about a metre of turbulent liquid.

2. LBCG

2.1 Program Structure

The LBCG program was designed with the following aims :

(i) To be usable on computers with basic word lengths varying from 16 to 60 bits.

(ii) To make best use of the core storage available.

(iii) To be as efficient as possible in the off-line mode, but if possible to design a data and program structure which could also be adapted to on-line use.

(iv) To allow the use of backing storage (e.g. drum or disk) if available.

(v) To make the program as modular as possible.

The result of these design criteria is a program written in strict ASA FORTRAN and using a linked block structure built up in blank COMMON for the storage of the principal data in the program. Further features are that the structure has been limited to a tree form for simplicity and convenience. A block may be defined to be of any length up to 32767 words (i.e. $2^{16} - 1$) and the blocks may be placed in any order within core, provided only that all linkages are forward in core. A simplified diagram of the tree structure used in LBCG is shown in Figure 4.

The input format to LBCG consists of the branch of the tree which commences at the FRAME block. As can be seen from Figure 5 both Title and Run Card information are also stored in the same form. As the geometry program proceeds it creates new blocks which describe the fits that have been performed. In addition, the linkages between blocks give information about the topology of the event, both in space, and in the projections.

The variable length blocks have the advantage that space is not wasted by many arrays being maximally dimensioned. The lack of restrictions in ordering of the blocks allows great flexibility in on-line measurement techniques and in the writing of the program modules.

It was envisaged that the program would run on some computers where the word length of integers and floating point numbers may be different. An example of a typical block is shown in Figure 5. It will be seen that most integers are packed either as four 8-bit quantities or as two 16-bit quantities. Alternatively integers may be stored in floating point form.

The blocks are manipulated by a set of utility routines in a manner analogous to that of many list processors. This inevitably

creates an overhead in the computation time (perhaps 5% of the total event processing time) but this is balanced by the greater efficiency made in the use of the core.

The program is divided into modules (or "processors"). Each processor uses only data in the linked block structure and provides as output further blocks in the structure. It is a strict rule that processors may communicate with each other only in this way. Thus the linked block structure may be considered as a pseudo input-output device. This has the consequence that it is extremely easy both to run LBCG in overlay form, or to stop the program at any point, write out the block structure and continue processing on another computer. Working space requested by a processor is allocated in a dynamic manner; the design is such that the matrices can be handled, if necessary, in double precision without disturbing the rest of the program.

One of the disadvantages of coding dynamic data structures in FORTRAN is that the readability of the coding deteriorates very quickly. A typical statement, loading a variable into a newly created block, might be Q(LMDF+18) = P, where Q represents the area for the linked blocks. The only means of identifying such statements is through the index LMDF. A complete set of mnemonics has been defined for all such variables referring to blocks in the LBCG structure. These mnemonics have been rigidly adhered to. In the example above the mnemonic stands for Location of Mass-Dependent Fit block.

The program also contains debugging routines which provide automatic print-outs of the block structures and all associated COMMON blocks. This is an important feature for list-structured programs.

Error messages have been concentrated in one routine which can, if necessary, be replaced by a dummy routine to save space.

The LBCG program and all ancillary programs have been constructed as a "PAM-file" under the update program PATCHY developed at CERN. This allows users to introduce special features associated with a given chamber, measuring machine etc. Certain options have

already been coded. These include conversion patches for different computers (e.g. IBM 360) and options for Gargamelle, Mirabelle and BEBC.

2.2 Smoothness Checks on Views

The methods used in classical chambers have been based on the fact that the projected track images are extremely well approximated by circles. However, it is clear that for large chambers this assumption can no longer be made. Work is continuing on trying to find techniques more applicable to large chambers. This may involve requesting measurements of "special points" such as cusp or loop points, in addition to physical points such as kinks.

2.3 Light Ray Calculations

Up to now, only test data from the artificial events program described in paragraph 3.1 have been used. This assumes a very simple pin-hole optical model. The coordinates are given by a measuring machine and have to be transformed into the film plane system; the method for doing this is to use camera-based fiducials. In real life, the lenses will be represented by a more complicated function, but this is only a serious problem for the calibration program which actually finds the function (see paragraph 3.2).

Finally, the light rays which have now been found in a coordinate system tied to the given camera, have to be transformed into the system of the chamber. Light rays are thus given in the chamber by the coefficient of $X = F_x Z+G_x$

$$Y = F_y Z+G_y$$

This last transformation is a simple one, once the position of each lens system is known with respect to the chamber. This problem is discussed in paragraph 3.3.

2.4 The computation of space points from the measurements

Two alternative processors have been written to compute the space points used to find a first approximation to a final fit. The

first, known as "Near Corresponding Points" (or NCP) is an extension of the techniques used in THRESH, while a new method known as "Quasi-Corresponding Points" (or QCP)[1] has been developed in an attempt to provide reliable errors and correlations on the space points.

The NCP processor, which finds space points by an interpolation technique, is more complicated in large chambers because tracks are longer and turn through large angles, and at the same time are viewed over wide range of angles. Both these effects contribute to the fact that track images on the film plane are far from circular and may contain loops or cusps. These give rise to geometrical ambiguities when trying to interpolate a given light ray from one view into another (see Figure 6). An algorithm has been developed, using circles as a local approximation to the track image, which resolves these ambiguities in most cases. Exceptional cases can arise if a section of the track is visible in only two views. Any unresolved ambiguities are finally removed by smoothness tests. Both Gargamelle and Mirabelle contain regions of the chamber, particularly at the extremities which are only visible in two views. A method has also been found to calculate errors associated with the near corresponding points but it is not possible to find the correlations between them.

The QCP processor was developed primarily for use with a new fitting technique (section 2.7) which uses the space points rather than the original measurements. However, apart from the correlations, the NCP and QCP processors are in principle interchangeable. (See Fig.7).

QCP approximates the track by local helices in space. For this purpose the tracks are divided into space segments and a local helix fit is performed on the film. It is assumed that each segment is sufficiently short to ignore magnetic field variation, energy loss and multiple scattering. A space point with errors is computed at the end of each segment. A series of fits, using non-overlapping segments is performed, each fit using the results of the previous segment as starting values. Work is continuing on trying to reduce the computation time of QCP.

2.5 Hydrogen Final Fit

In the same manner as for classical chambers, a helix is fitted to the near corresponding points to serve as a first approximation. Then the parameters are improved by making an iterative least squares fit of the track to the light rays, for each mass separately.

As well as the parameters of the helix, the first approximate fit must also give the arc lengths of a point on the helix adjacent to each light ray. For a light ray which gives a near corresponding point, this is easy. For a light ray which does not, its point of intersection with a ruled surface containing the helix is found; the technique here has had to be changed because of the wide angle of the light rays.

For the final fit itself, the assumption is still made that the measurement errors (or root mean square deviations of measured points from the track) are the same for all measurements on all views and are uncorrelated. The only problem with the new chambers is in the calculation of the weighting factor w by which a given space displacement D is multiplied in order to project it into a film deviation d.

Referring to Figure 8 it can be seen that $\vec{D}$ which is in a plane P perpendicular to the light ray can be projected to the distance d_1 in the film plane. This is done simply and generally on the assumption that the demagnification to the film plane from the plane P can be represented in the vicinity of $x_f y_f$ by two demagnification components (1) m_r along a line joining $x_f y_f$ to the foot of the optic axis (0,0) and (2) m_t perpendicular to this. A further factor is required to take account of the fact that in the film plane the projection of $\vec{D}$ is not perpendicular to $\vec{n}$, the projection of the track tangent $\vec{T}$, i.e. the distance d is required, not d_1.

It has been found from a sample of artificial events, that in the case of BEBC with pin-hole optics, use of this more complicated weighting function gives correct results, with fewer iterations. (With Mirabelle and pin-hole optics, it gives exactly the same results as

the THRESH formula). It now remains to find ways of reducing the computation time.

Two other sources of error which could be taken into account when fitting tracks in hydrogen are (1) multiple scattering (2) errors in camera positions. Ways are being investigated for dealing with the first, but so far they require large amounts of computer time. The problem of incorporating the second has not yet been looked at seriously.

2.6 Heavy Liquid Final Fit

An alternative method for estimating the initial track parameters has been coded for LBCG which is particularly suited to heavy liquid tracks, and is therefore commonly referred to as "The Heavy Liquid Fit" [1].

The essential philosophy is that uncertainties due to multiple scattering and bremsstrahlung be included with measurement error in the 'a priori' covariance matrix of a least squares fit to the space points. In more traditional methods, these physical effects are neglected during the fit, and are taken into account only in an external assessment of the errors on the track parameters. In heavy liquids this approach may lead to convergence difficulties, and necessitates special techniques such as "Optimum length" to avoid serious over-estimation of errors.

The space points are fitted to a mean trajectory, which takes into account energy loss and magnetic field variation, and is generated in a step-by-step manner, using local approximate spirals. Six parameters, $\frac{1}{p_o}\ \lambda_o\ \varphi_o\ X_o Y_o Z_o$, are fitted for a given mass, and the redundant parameter is eliminated by an internal constraint on the space arc lengths.

The fit is made to the deviations of all points in two directions perpendicular to the track (normal and binormal) and to the tangential displacement of the initial vertex. N space points therefore imply (2N+1) measurements, and a covariance matrix of size (2N+1) x (2N+1). A special technique, critically dependent on the

representation of the error propagation, is used to avoid direct inversion of this matrix. This technique takes advantage of the tri-diagonal form of various intermediate matrices, and gives a calculation time proportional to n(=2N+1) rather than the more typical n^3.

The information that a track stops may be introduced as a direct constraint in the fit. The mean trajectory is adjusted to give zero momentum at the end point by changing the energy loss along the track relative to the errors of straggling and range measurement. This gives an extra term in χ^2 which represents the discrepancy between the fitted momentum and the range of the track. Straggling errors are included as an extra table in LBCG, and the range errors are given by QCP.

Although the fit is mass-dependent, choosing between different mass assignments is complicated because the error matrix varies with mass. It is necessary to normalise the χ^2s in a complex manner, and so far this problem has not been fully resolved.

A pre-fit over the first part of the track, neglecting off-diagonal error terms, speeds up the full fit and provides sufficiently good starting values so that the full error matrix need be computed only once.

Preliminary results from a first version are encouraging and large scale tests with real and artificial data will follow.

2.7 Track Matching and Bridging

The matching problem is more severe in large chambers for the following reasons.

i) The wide angle lenses give rise to projected curvatures in each view which are not at all comparable.

ii) A given track may appear in any arbitrary number of views from two to eight.

iii) For Gargamelle and Mirabelle each view sees only a portion of the chamber. This implies that in some views tracks will be seen without their associated vertices. The problem of correctly associating these "hanging" tracks has become known as "bridging". A good example is seen in Figure 2.

iv) The computation of near corresponding points needed for one of the techniques currently used in classical chambers for the production of estimators [2] is much more complicated in large chambers (see section 2.4). In addition, geometrical ambiguities exist for a single track which make the use of such points as estimators for the "goodness of match" rather dubious.

The present version of the program provides matching of the vertex points (a new feature not normally necessary for classical chambers), followed by matching of the tracks visibly attached to a vertex. The final step of "bridging" the "hanging" tracks has been designed but not yet coded. This step would, of course, be unnecessary for chambers such as BEBC.

It was felt worthwhile to concentrate first on a matching technique using relatively simple tests, which tries to reduce to a minimum the number of unresolved ambiguities for which a final fit must be called. In particular all acceptable doublet matches are combined immediately into possible multiplet matches, rather than producing intermediate lists of triplet, quadruplet matches etc. It is clear that such a processor will be extremely useful for partially automatic devices such as ADAM + EVA or DOLL [3], for which versions of LBCG may be operating in an on-line mode.

Doublet matching is done first on the basis of the space tangents at the vertex, followed by the estimation of the curvatures in an orthogonal projection. The curvatures computed in the reference plane were found to be completely unreliable due to the rapidly varying magnification. A new feature is that the track parameters are retained with the doublet, and subsequently with all multiplets.

These could in principle be used as a first approximation of the final fit.

The list of multiplet matches (i.e. in which all possible pairs are compatible) are built up directly from the doublets using the track parameters for compatibility tests. At the moment fixed tolerances are used for this purpose, but it is hoped to introduce some error computation to make this more flexible. The sole "estimator" used for a multiplet is its multiplicity, higher order multiplets always being taken in preference to lower order multiplets whenever there is a clash. This rather crude test has proved to be very effective in removing spurious multiples from the simulated 6 GeV/c 6-prongs in Gargamelle studied so far.

It is envisaged that the bridging problem may be solved by estimating the track parameters through a crude, local helix fit on the views in which the vertex is visible, and then projecting the results into the views containing the "hanging" tracks.

It remains to be seen how successful these techniques will be in eliminating the need to call for a final fit in order to be sure that a given multiplet is really a correct match. It is hoped that on devices such as ADAM + EVA, there will be fewer problems with beam tracks, but it is expected that there will always be a residue of ambiguities for which a fit is necessary.

3. Ancillary Programs

3.1 Artificial Event Generation

Since existing programs, such as WORM, were found to be inadequate for large chambers, a new program called GAT has been written. This program is designed to provide artificial data to study scanning and measuring problems, and to provide test input for geometry programs in the absence of real data. GAT has been developed from a combination of two earlier programs known as FOWL and

WORM. Several approximations made in WORM have now been removed, and the program will now provide tracks which include the effects of energy loss, multiple scattering and bremsstrahlung.

The present version of the program can be used for either classical or new bubble chambers. A reduced version of GAT (VAT69) is also available on the CERN CDC 3100 computer as an interactive program using the CDC 250 display. Thus different measuring techniques may be studied by selecting special tracks and indicating measurements using a light pen. The data is then analysed using LBCG off-line on the central computers.

GAT has four distinct processors, not all of which need to be selected. These are :

REACT To trace a beam particle through the chamber until it undergoes a reaction specified by the user, and then to compute the kinematics of the event according to Fermi's statistical phase space.

SPACE To compute a series of space points along the secondary particle tracks by Runge-Kutta integration, including, if requested, energy loss, multiple scattering and bremsstrahlung.

PROJCT To project the track points to simulated cameras. The optical model may be either a simple pin-hole model or a complicated calibration function.

PLOT Provides plots of the generated events in the film plane.

These processors are rather independent and it is possible to use only certain combinations of them. In particular, it is possible to display the output from the SPACE processor on the CDC 3100, thus avoiding the time-consuming track generation part of the program.

3.2 Calibration of Lenses

The calibration of the lens systems is an important problem which has received much attention. The Gargamelle and Mirabelle lenses are currently being calibrated at CERN and Saclay respectively.

Theoretically the lenses in all three chambers are axially symmetrical and have the radial distortion patterns shown in Figure 9. In addition to this the entrance pupil moves 0.9mm in Gargamelle and 2mm in Mirabelle, as the viewing angle goes from 0^{o} to 55^{o}.

The Gargamelle lens systems are being calibrated on an optical bench. A pair of parallel glass plate grids are photographed through each lens and camera unit. A least squares fit of the image space coordinates to the object space coordinates is made, with respect to as many parameters as are found necessary to reduce the residuals to acceptable values. Preliminary results show close agreement with the theoretical radial distortion, but also that it is necessary to introduce tangential distortion terms. It is hoped that only a simple correction term is required in order to transform from air to liquid in the object space.

The Mirabelle lenses on the other hand, are being calibrated while mounted on the filled chamber. The object space reference frame consists of (a) the steel rulers marked with crosses and (b) a plane of parallel wires strung with small beads (see Figure 10). In the fit, the relative positions of the beads are known precisely, as are the relative positions of the crosses. In neither case are the positions with respect to the lens camera system assumed known. The lenses of BEBC will also be calibrated on the chamber, probably using laser lines in addition to the crosses.

3.3 Reconstruction of Camera Positions

The assumption is made that each camera and lens system is a completely rigid unit, and a coordinate system (xyz) is associated with each such unit. The position of each such set of axes relative to the chamber system can be defined by the coordinates (XYZ) of the origin and three rotations (ψ, φ, θ). The only method of finding these six parameters to sufficient precision is to measure the film images of a large set of fiducial marks in the chamber, and to make a least squares fit taking all views together.

Following the work of P. Negri [5], a photogrammetry technique is used. The basic method is to minimise the sum of squares of distances between all pairs of light rays corresponding to the same fiducial mark, taken over all fiducials and views. This method does not require the positions of the fiducials to be known, but does give the result in the coordinate system of one of the cameras. A second much simpler fit is then made to transform the result into a coordinate system defined by some of the fiducials.

In the current version of the EEL program, the two fits are combined into one.

Unfortunately it is not possible to calculate the full error matrix in the case where more than three views of the same fiducial are taken together. However, better results have been found using all measurements and ignoring correlations than restricting to triplets with full error matrix (see Figure 11). The reliability of the errors furnished by the program has been tested by running with sets of artificial data in which the measurements have been randomly varied within their error.

The program can also make use of measurements on laser lines in the chamber. It has been shown that use of measurements of point objects or laser lines in the chamber, in addition to those of fiducials on the walls, improves the precision of the fit (see Figure 12). Up to now a pin-hole optics model has been assumed for the artificial data, but the more general case can be treated in the EEL program.

It remains to be seen whether the camera positions really remain as stable from expansion to expansion as has been predicted. There may be the additional problem with Gargamelle and BEBC that the camera and lens systems do not behave as a rigid unit.

3.4 Estimation of the Magnetic Field

Preliminary information indicates that the homogeneity of the magnetic fields will probably be rather poor compared with the CERN 2-metre Chamber and for Gargamelle and perhaps Mirabelle one will not be able to neglect the x and y components of the field.

Some 2000 preliminary measurements[4] have been taken for Gargamelle. These indicate the z component has a mean value of about 16.5KG with a variance of 4KG. The x and y components are expected to have mean values of 1KG and 0.5KG respectively.

A least squares fit was made to the z component of the field, taking advantage of the intrinsic symmetries of the magnet and Maxwell's equations. Using 30 parameters an overall fit for the whole chamber gave a mean residual error of 1% compared with an estimated precision of 0.1% on the measurements.

It is clear that the boundary regions give rise to a large number of additional coefficients in the fit, and work is continuing on examining the possibilities of using overlapping fits or using a fit combined with a table in order to reduce the computation time.

4. Conclusions and Future Plans

Work on a reconstruction program for the new large bubble chambers is in an advanced state. The structure of the program is such that it can easily be adapted to most scientific computers, and also its modular structure allows easy insertion of alternative numerical methods.

An interface with the existing kinematics program is being written. However, the LBCG program will ultimately be converted to the more general HYDRA linked block structure [6], which is being designed as the standard for the complete chain of processors to be used in bubble chamber film analysis. Conversion to the HYDRA structure should not present any serious problem, and will have the advantage of providing a unified complete analysis chain and not just a geometry program.

Acknowledgement

We would also like to acknowledge the indirect contributions and moral support of many other collaborators, too numerous to name individually.

References

1. C. Pascaud, D. Morellet.
"Essai de géométrie originale resolvant les problèmes des chambres à bulles géantes" L.A.L. 1227 Orsay, January 1970.

2. J.M. Gerard, W. Krischer, D.O. Williams.
"The CERN Track Match Program for Vertex Guidance Bubble Chamber Measurement Systems", Proceedings of the International Conference on Advanced Data Processing for Bubble and Spark Chambers, Argonne, ANL-7515, pp. 431-443. Oct. 1968.

3. J. Altaber et al.
"ADAM + EVA, a universal scanning and measuring machine for film from the large bubble chambers". CERN Report DD/DH/70/7, March 1970.

4. R. Grüb, J.M. Maugain.
"Magnetic Field Measurements in the Gargamelle Bubble Chamber Magnet" NPA/Internal 69-5, May 1969.

5. P. Negri.
"Reconstruction of Fiducial Marks and Cameras utilising simultaneously all the Photographs available".
Rev. Sci. Instr. Vol. 40 (1969) pp. 148 - 154.

6. R.K. Böck, H. Burmeister, W.G. Moorhead, E. Pagiola, M.C. Turnill, J. Zoll.
"The Future of Track Chamber Programs at CERN". CERN Report DD/DH/69/5, June 1969.

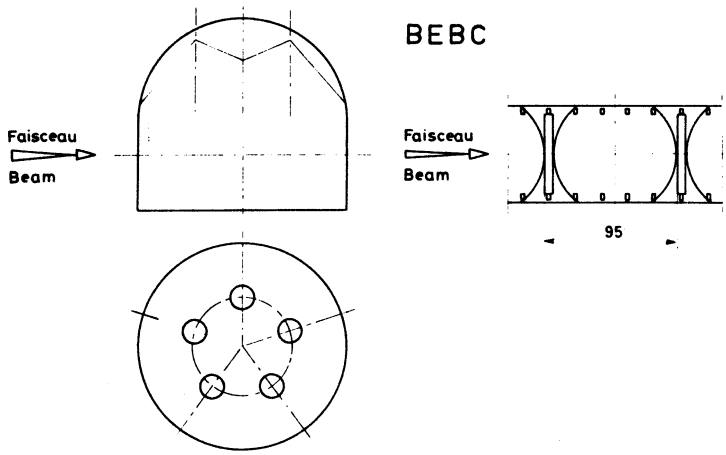

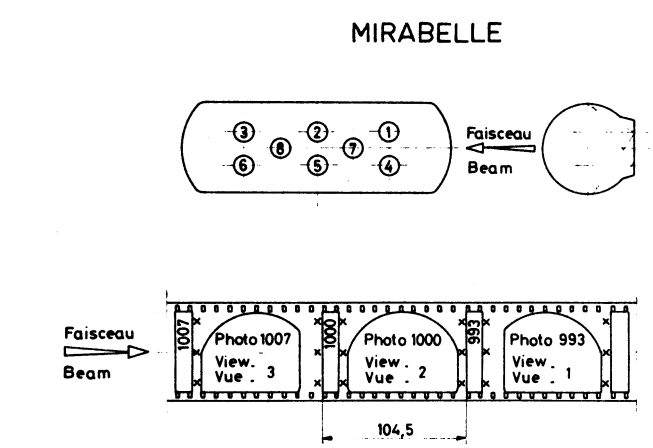

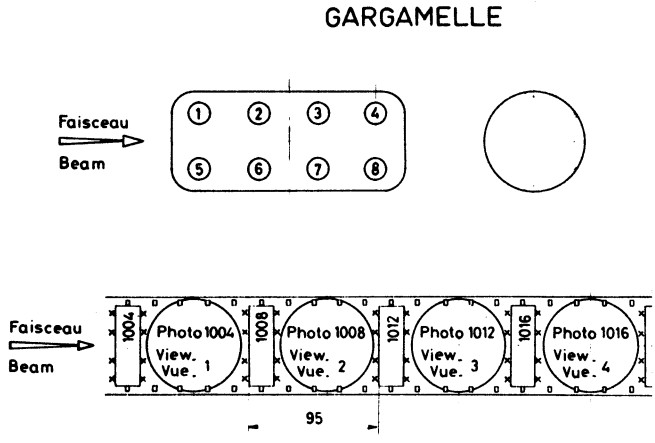

Schematics of BEBC, Gargamelle and Mirabelle

Fig. 1

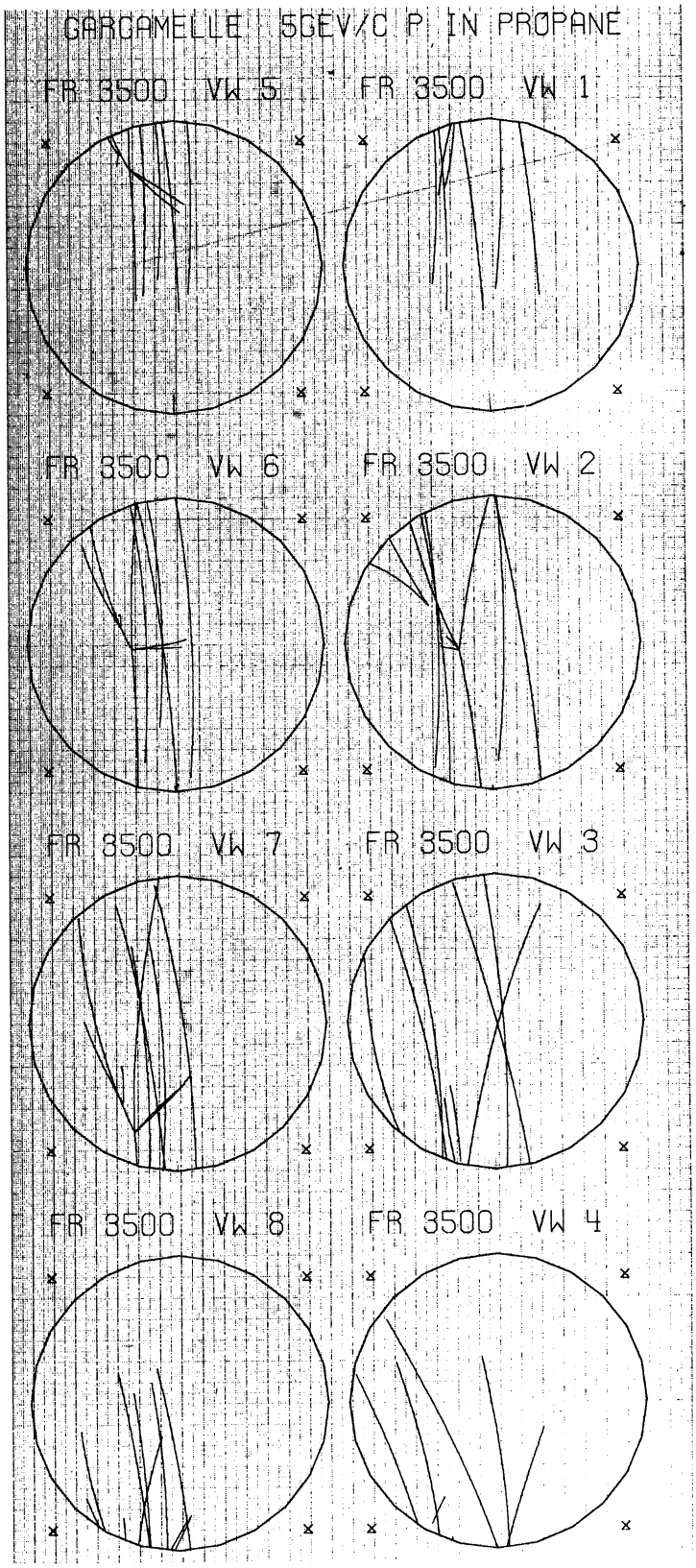

Artificial Event in Gargamelle

Fig. 2

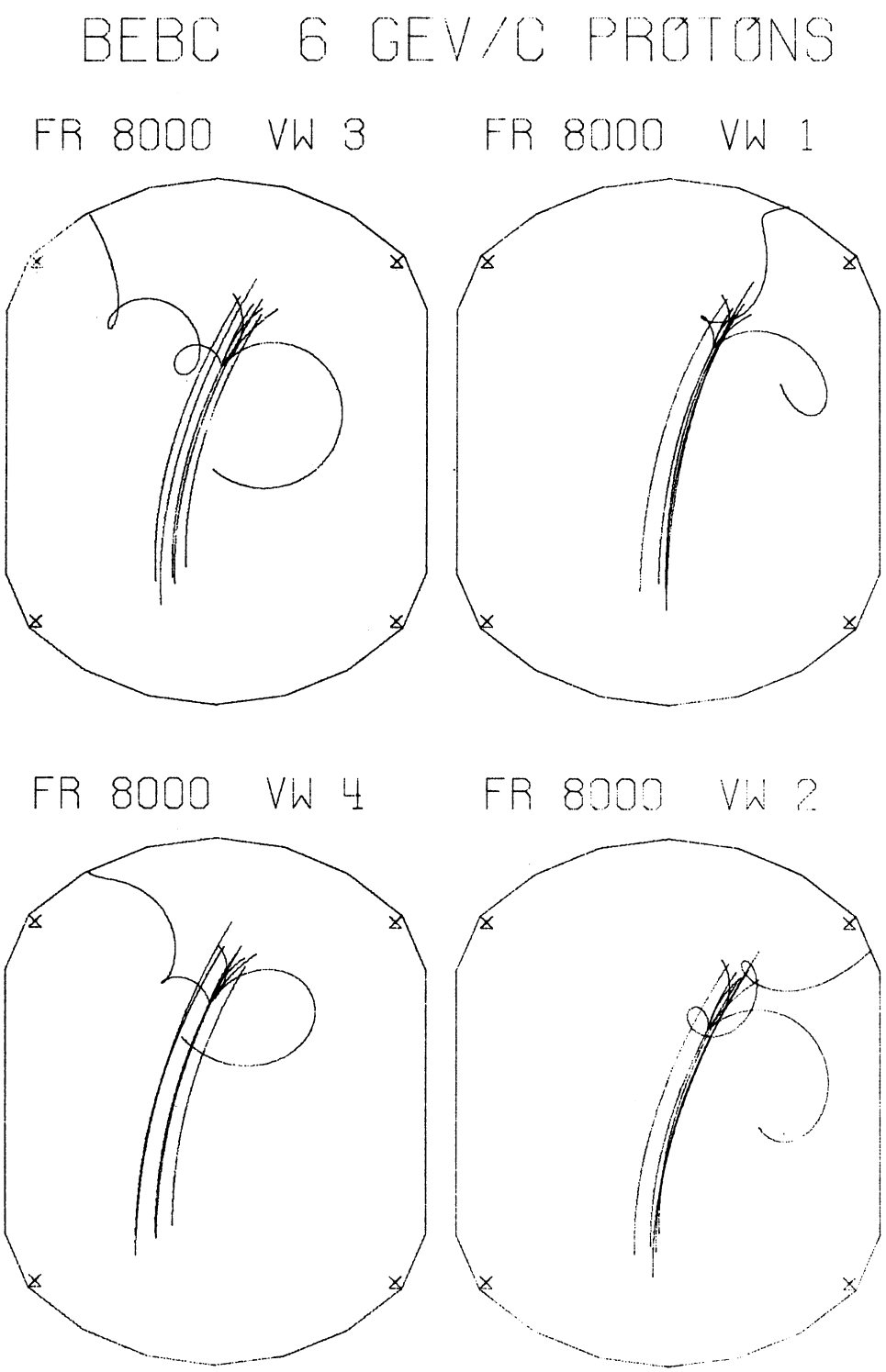

Artificial Event in BEBC

Fig. 3

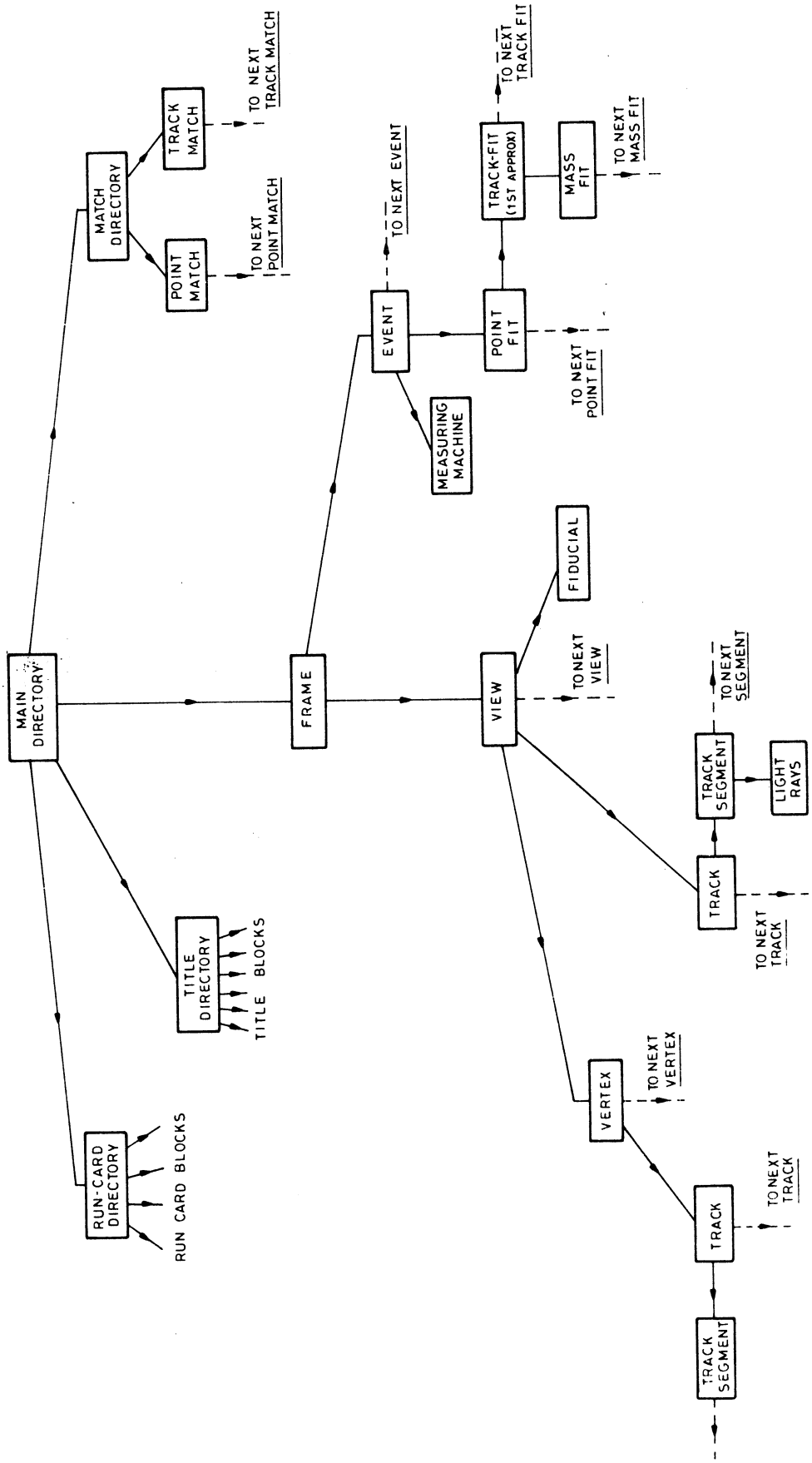

LBCG TREE STRUCTURE

Fig. 4

CONTENTS OF TRACK-SEGMENT BLOCK

Word		
0.	1.	Number of words in block
	2.	Location of next track-segment block
1.	1.	Block type number
	2.	Fault code
	3.	Type of co-ordinate storage (= 2 for floating-point)
	4.	Start of co-ordinate storage = 6
2.	1.	Not in use
	2.	Location of comment block (if any)
3.	1.	Type of segment
	2.	Number of co-ordinates
	3.	Number of co-ordinates used in fit*)
	4.	Number of special points
4.	1.	Measuring-machine number
	2.	Scan number (reserved for HPD)
	3.	Re-measurement number
	4.	Direction of segment
5.	1.	Location of space-distance block*)
	2.	Location of light-ray block*)
6F. onwards.	X Y	} pairs for each point

*) Filled in by LBCG

Typical Block in LBCG

Fig. 5

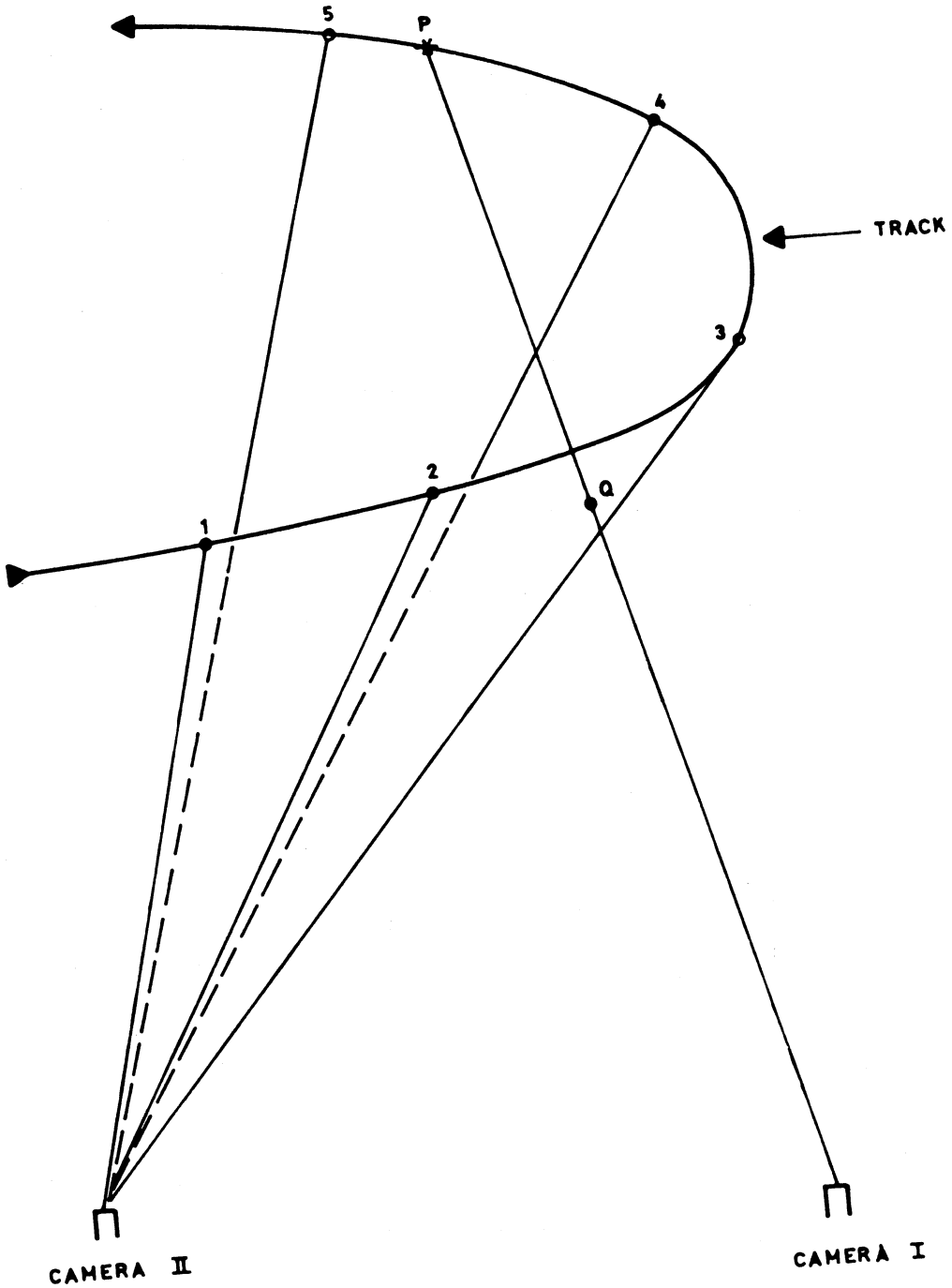

Geometrical ambiguity found during Near Corresponding Point Computation

Fig. 6

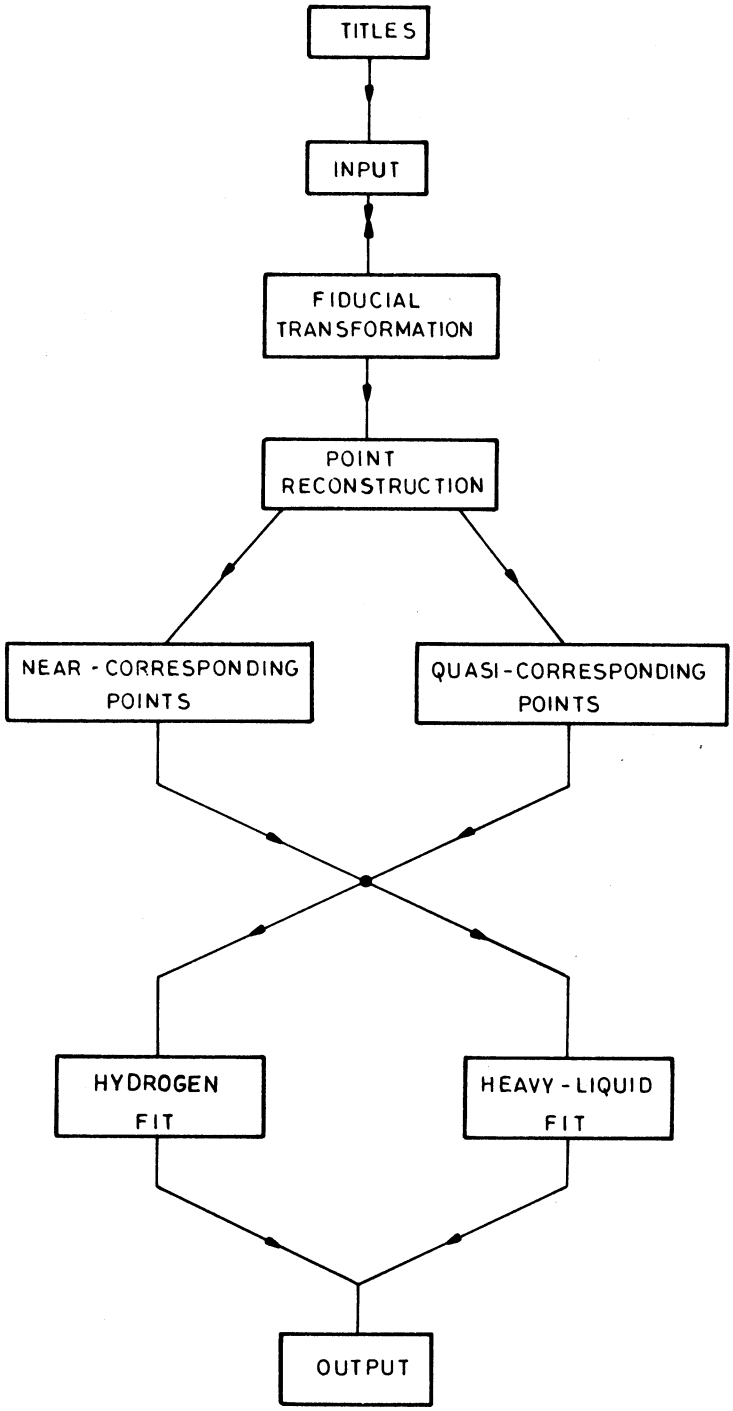

MODULES (OR PROCESSORS) OF LBCG

Fig. 7

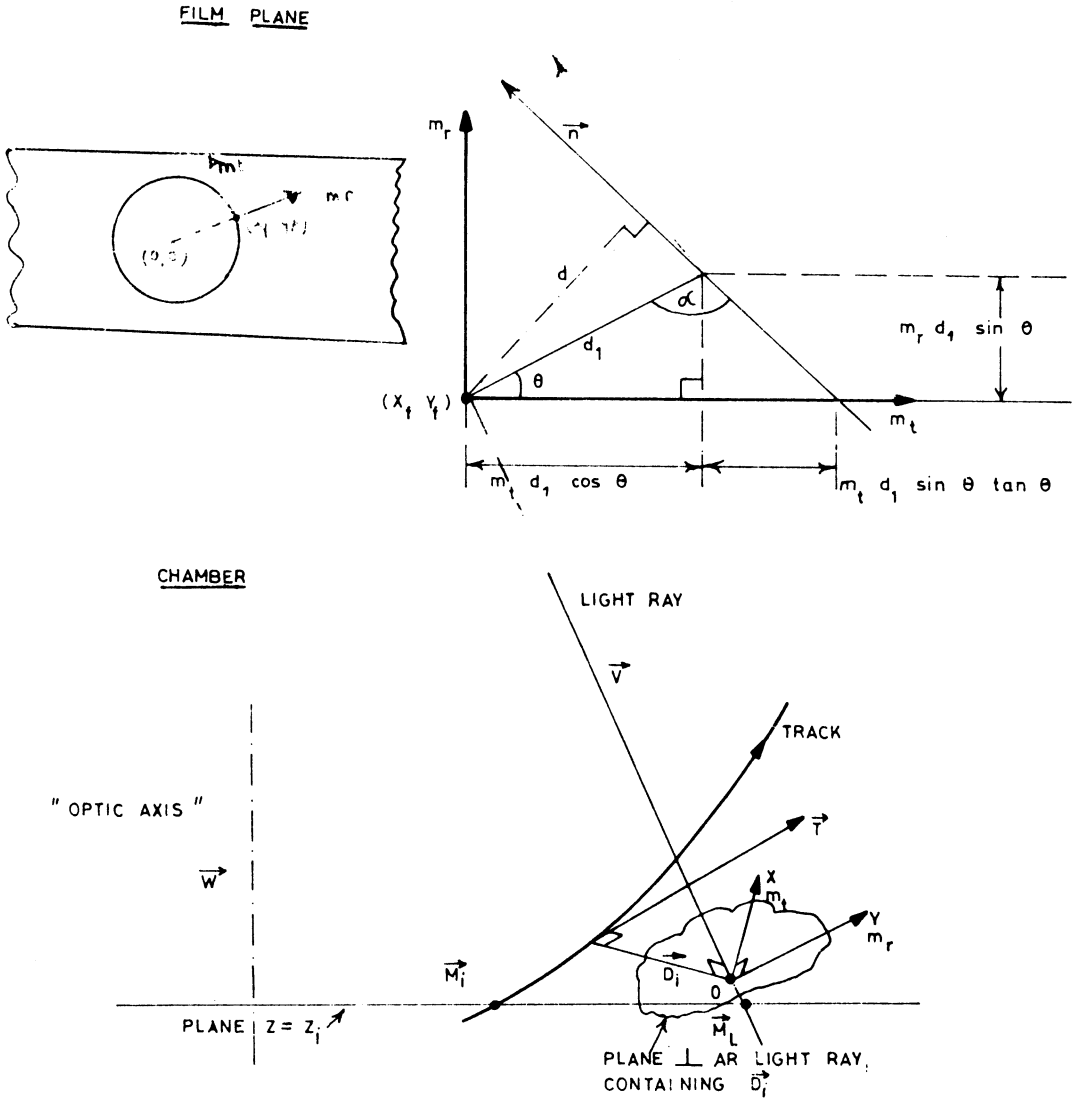

Transformation from Space to Film

Fig. 8

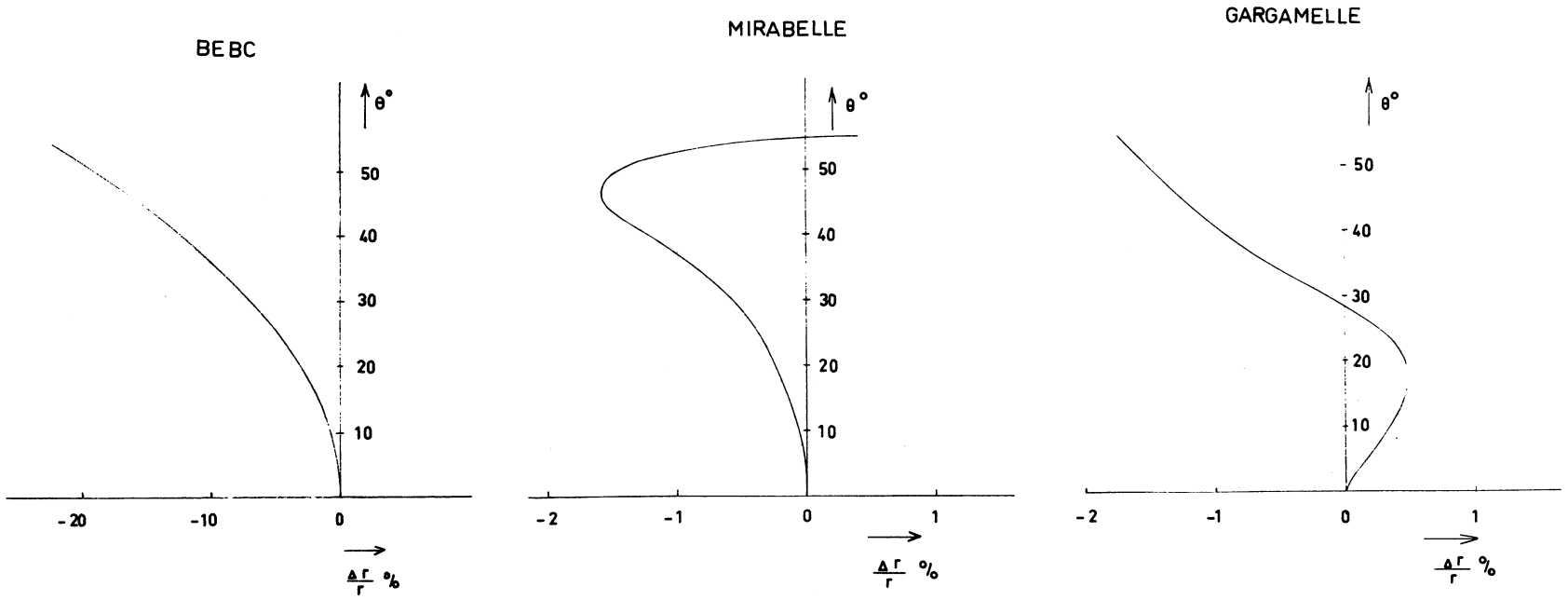

Theoretical Radial Distortions

Fig. 9

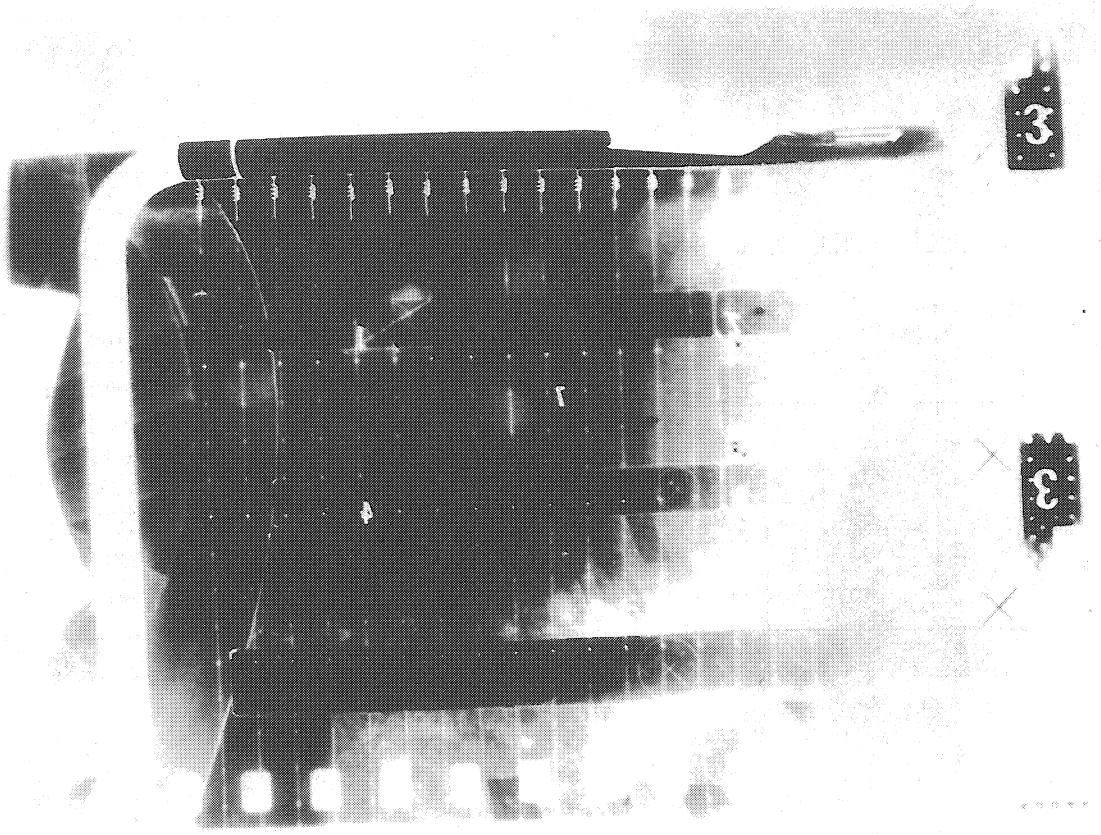

The Calibration Beads in Mirabelle
(View 7)

Figure 10

Reconstruction precision of camera positions

Procedure with triplets

Number of floating fiducials	Number of equations	Outermost cameras						Innermost cameras					
		Δx	Δy	Δz	$\Delta\psi$	$\Delta\varphi$	$\Delta\vartheta$	Δx	Δy	Δz	$\Delta\psi$	$\Delta\varphi$	$\Delta\vartheta$
16	48	0.84	1.78	1.32	1.25	0.37	0.52	0.70	0.70	0.45	0.46	0.15	0.24
20	54	0.97	1.77	1.34	1.26	0.42	0.60	0.75	0.71	0.47	0.48	0.15	0.24
24	69	0.64	1.11	0.77	0.78	0.27	0.37	0.61	0.61	0.37	0.42	0.14	0.22
28	84	0.58	0.82	0.58	0.58	0.23	0.33	0.55	0.57	0.36	0.40	0.12	0.20
32	No convergence for this particular set of fiducials												

Procedure with complete diagonalized matrices

Number of floating fiducials	Number of equations	Outermost cameras						Innermost cameras					
		Δx	Δy	Δz	$\Delta\psi$	$\Delta\varphi$	$\Delta\vartheta$	Δx	Δy	Δz	$\Delta\psi$	$\Delta\varphi$	$\Delta\vartheta$
16	310	0.38	0.65	0.51	0.43	0.12	0.21	0.35	0.44	0.26	0.30	0.09	0.14
20	350	0.37	0.62	0.48	0.42	0.11	0.19	0.33	0.42	0.25	0.28	0.09	0.13
24	404	0.33	0.50	0.37	0.33	0.10	0.16	0.30	0.38	0.23	0.26	0.09	0.12
28	416	0.32	0.47	0.34	0.31	0.10	0.16	0.30	0.38	0.23	0.26	0.08	0.12
32	476	0.31	0.46	0.33	0.31	0.10	0.15	0.29	0.37	0.22	0.25	0.08	0.12

Δx, Δy, Δz in mm, $\Delta\psi$, $\Delta\varphi$ and $\Delta\vartheta$ in mrad.

Fig. 11

Points in the chamber

Number of floating fiducials	Number of equations	Outermost cameras						Innermost cameras					
		Δx	Δy	Δz	$\Delta\psi$	$\Delta\varphi$	$\Delta\vartheta$	Δx	Δy	Δz	$\Delta\psi$	$\Delta\varphi$	$\Delta\vartheta$
32	476	0.31	0.46	0.33	0.31	0.10	0.15	0.29	0.37	0.22	0.25	0.08	0.12
32	394	0.27	0.36	0.29	0.24	0.09	0.13	0.26	0.32	0.20	0.22	0.08	0.11

Application of lasers

Number of floating fiducials	Number of equations	Outermost cameras						Innermost cameras					
		Δx	Δy	Δz	$\Delta\psi$	$\Delta\varphi$	$\Delta\vartheta$	Δx	Δy	Δz	$\Delta\psi$	$\Delta\varphi$	$\Delta\vartheta$
16	310	0.38	0.65	0.51	0.43	0.12	0.21	0.35	0.44	0.26	0.30	0.09	0.14
16	402	0.34	0.41	0.36	0.27	0.11	0.18	0.31	0.30	0.21	0.22	0.08	0.12

Fig. 12